



25th ABCM International Congress of Mechanical Engineering
October 20-25, 2019, Uberlândia, MG, Brazil

COB-2019-1131

FLUID–STRUCTURE INTERACTION SIMULATION OF MARINE STRUCTURES

Renata Ferreira Martins Rocha

Hélio Ribeiro Neto

Pedro Ricardo Corrêa Souza

Aristeu da Silveira Neto

Aldemir Aparecido Cavalini Junior

João Marcelo Vedovoto

School of Mechanical Engineering, Federal University of Uberlândia, Av. João Naves de Ávila, 2121 Bloco 5P, 38400-902 Uberlândia, Minas Gerais, Brazil

renatarocha@ufu.br

helio.ribeiro@ufu.br

eng.pedro.ricardo@gmail.com

aristeus@ufu.br

aacjunior@ufu.br

vedovoto@ufu.br

Abstract. *This paper presents numerical fluid–structure interaction (FSI) simulation of a pluck test applied to a Spool structure submerged in sea–water. The Navier–Stokes and mass conservation equations are solved in a Structured Adaptive Mesh Refinement (SAMR) framework used for fluid domain calculations and a Timoshenko beam finite element is used for the solution of displacements and velocities of the Spool structure. The coupling between fluid and solid domains is possible due to the usage of Immersed Boundary Method (IBM) and the strong coupling algorithm for FSI. The resulting computational fluid dynamic simulation with fluid–structure interaction is obtained using the in–house code MFSim. The pluck test in this context is emulated by a instantaneous force applied in a certain point of the structure, the displacement results influenced by the hydrodynamic loads are shown and discussed. An analysis of the FRF of the signal and the comparison between the natural frequencies in vacuum and water are shown. The results show the capabilities of the current methodology to estimate the natural frequencies of any beam structure surrounded by any fluid with only initial and boundary conditions, no adhoc constants or added mass methods are used.*

Keywords: *fluid–structure interaction, Spool, vibrations, fluid dynamics*

1. INTRODUCTION

Offshore pipeline structures are becoming increasingly problematic for engineers. It is common that these components are subjected to fatigue damage due to Vortex Induced Vibrations provided by the bottom currents and/or Flow Induced Vibrations by its internal flow rate Bruschi *et al.* (2015). Among this class of structures the subsea rigid jumpers (SRJs), also known as spools, are critical components that provide connection between well heads, manifolds or riser base and flowline end termination.

Under certain conditions, the spool vibration can be self–excited and its behavior becomes unstable. These instabilities and, more specifically, the conditions under which they emerge are very important to designers.

To fabricate this long pipe structures that essentially can not fail once in operation, the knowledge of its natural frequencies, once installed in deep sea is essential. Various methods for acquiring this frequencies under water are used in structural analysis, the most common one is the added mass. This method rely on empirically calibrated equations to provide a fictitious mass to be added in the solid, in order to emulate the fluid resistance to the structure's vibration.

This paper aims in presenting a method to determine the natural frequencies of any beam like structure submerged in any fluid only by imposing boundary and initial conditions. This is possible because both fluid and structure are solved with accurate and appropriated numerical methods. For the fluid domain, the Navier–Stokes and continuity equations are solved using finite volumes in a tree-dimensional SAMR mesh locally refined close to the spool structure. In order to account for the presence of solid body in the flow–field the IBM is used. The structure vibrations are found using a Timoshenko beam finite element. Both domains are coupled so that the displacement and velocities obtained by the finite element are passed to the fluid calculations and the hydrodynamic forces are sent back to the structure. This is done interactively in each time step by an algorithm called strong coupling.

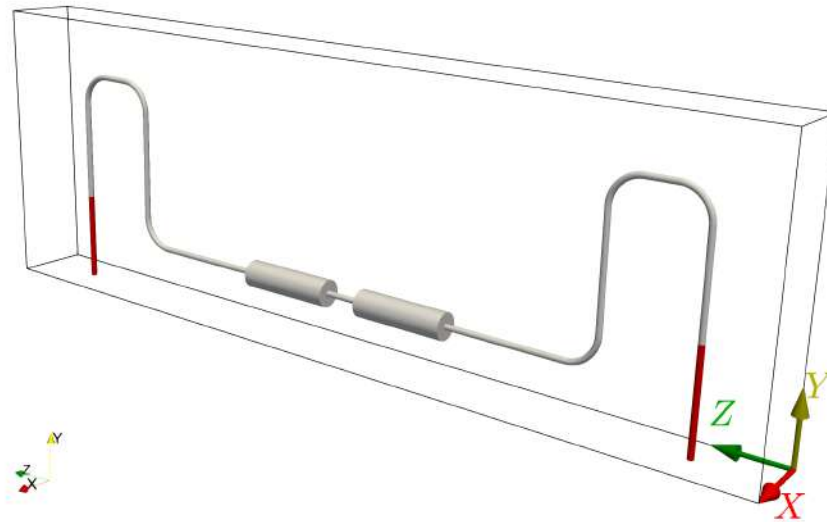


Figure 1: Fluid domain with the structure and sea bed modeled as flat wall. Fluid reference axes (X , Y , Z) visible.

2. METHODOLOGY

Spools may be subjected to sea currents which can induce fluctuations of the fluid dynamical forces that excite the structure.

The purpose of this section is to present the physical, mathematical, and numerical models used to simulate the problem of interest.

2.1 Physical model

In the physical model, the problem of interest is evaluated and physical assumptions are adopted to make the solution feasible. The assumptions for each subsystem will be presented separately.

2.1.1 Fluid subsystem

In this subsection, the physical assumptions for the fluid subsystem are presented. They are separated into three subgroups: domain, flow, and physical properties. The domain of the physical problem is the ocean, in which the structure is immersed. It is important to note that the domain is delimited by the seabed, which although static, influences the flow and, as a consequence, the vibration of the structure. Since the simulation of the ocean in all its extension is impractical, it is necessary to choose a reduced domain for the problem analysis. A domain with length 148ϕ , 16ϕ wide, and 50ϕ high was chosen, where, ϕ is the nominal diameter of the pipe.

An illustration of the fluid domain with the structure is presented in Figure 1.

The flow inside the structure is not considered. The internal fluid is modeled as a rigid body and accounted on the inertia and self-weight calculation of the structure. The external flow and its influence on the structure is considered. Initially the fluid is static, after the structure is excited by a instantaneous force, the fluid starts to move with the structure.

The initial and boundary conditions are important, since errors in these conditions can be amplified exponentially by nonlinear interactions, generating instabilities Damasceno *et al.* (2015). Any variation in the initial conditions may determine different states.

The physical properties of the fluid are considered constant. In addition, it is assumed that saltwater behaves as a Newtonian fluid. The dynamic viscosity was held at $\mu = 1.62 \times 10^{-3}$ Pa s and the density at $\rho_f = 1.025 \times 10^3$ kg m⁻³.

2.1.2 Structure subsystem

The physical and geometrical properties of the Spool will now be presented. The Spool is attached to pipes used for oil and natural gas transportation, that can be kilometers long. However, the calculation domain must be reduced to enable numerical simulation. Therefore, the domain chosen for the structure subsystem has length 123.5ϕ . The pipe has a circular section of external diameter ϕ and internal diameter $\phi_i = 0.843\phi$ m, which are constant.

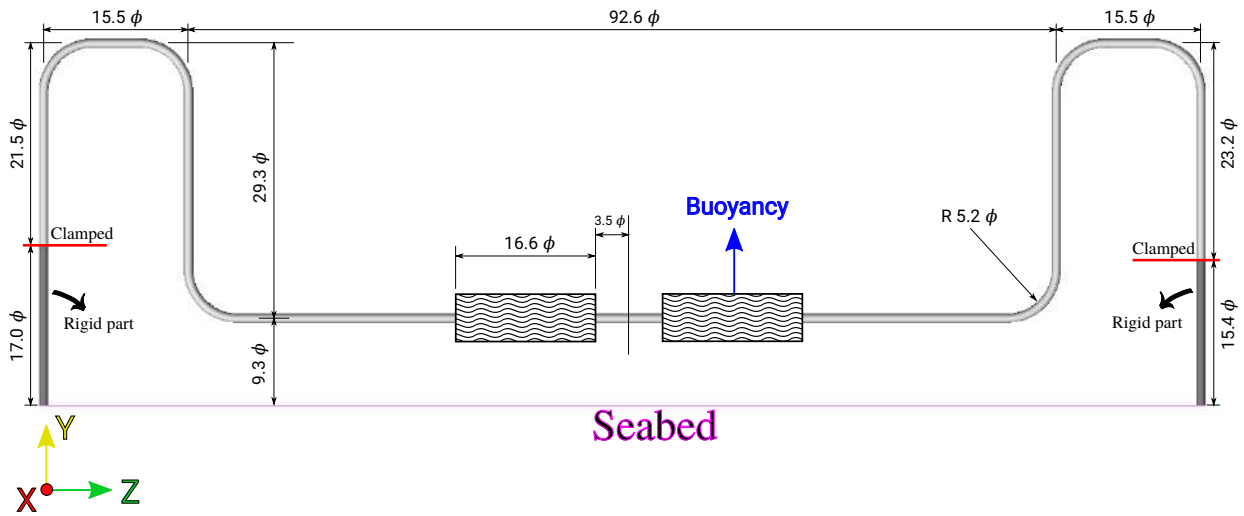


Figure 2: Spool's geometry illustration.

The pipeline is made of steel and is covered with a layer of anti-corrosive material. The thickness of the layer of anti-corrosive material is $12\% \phi$. The pipe is also filled with oil. The layer of anti-corrosive and the oil are considered to be rigid bodies and are accounted in the effects of the inertia of the pipe and the self-weight calculation.

The physical properties of the structure are considered constant over the domain. It is assumed that the steel behaves as a linear material with modulus of elasticity $E = 2.07 \times 10^{11}$ Pa, Poisson coefficient $\nu_s = 2.9 \times 10^{-1}$. The steel density adopted is $\rho_s = 7.850 \times 10^3$ kg m⁻³.

External and internal fluid pressure causes a resultant traction axial force that increases the stiffness of the structure.

The geometry of the spool is illustrated in Figure 2. There are 2 floaters, that apply buoyancy forces to the structure. These floaters don't have a structural function, but one must take in to account their presence due to the buoyancy force and the hydrodynamic force.

A instantaneous force is applied to the structure in order to excite the structure on all its natural frequencies. The point where the force is applied and the position of the probe used are illustrated on Figure 3. The force is applied on the three directions, in order to excite all the modes of the structure.

2.2 Mathematical model

In this mathematical model, the differential equations take into account the simplifications discussed the physical model. The models for the fluid and structure subsystems will now be presented.

2.2.1 Fluid subsystem

For the fluid subsystem, the simplified mass balance equations for incompressible flow, and the simplified linear momentum balance equations for isothermal, constant physical properties, and incompressible flows were used. Equation (1) expresses the simplified mass balance equations for the case of incompressible flow in Cartesian coordinates, using Einstein's summation convention:

$$\frac{\partial u_j}{\partial x_j} = 0, \quad j = 1, 2, 3, \quad (1)$$

where x_j are the coordinate directions X , Y and Z , respectively, and u_j is the component of the velocity of the fluid in the direction j . Equation (2) expresses the balance of linear momentum for a Newtonian fluid written in divergent form, simplified for the case of constant specific mass and written in Cartesian coordinates:

$$\frac{\partial u_i}{\partial t} + \frac{\partial u_i u_j}{\partial x_j} = -\frac{1}{\rho_f} \frac{\partial P}{\partial x_i} + \frac{\partial}{\partial x_j} \left[\nu \left(\frac{\partial u_i}{\partial x_j} + \frac{\partial u_j}{\partial x_i} \right) \right], \quad (2)$$

where $i, j = 1, 2, 3$, P is the pressure, and t is the time.

Equations (1) and (2) are considered sufficient for the simulation of the fluid dynamics of the flows of interest.

The initial and boundary conditions used are shown in Table 2 and Table 1, respectively.

In addition to the boundary conditions described in Table 1, it is necessary to set the fluid boundary condition at the interface between the fluid and the structure. An imposed velocity condition (Dirichlet) was employed. The fluid velocity

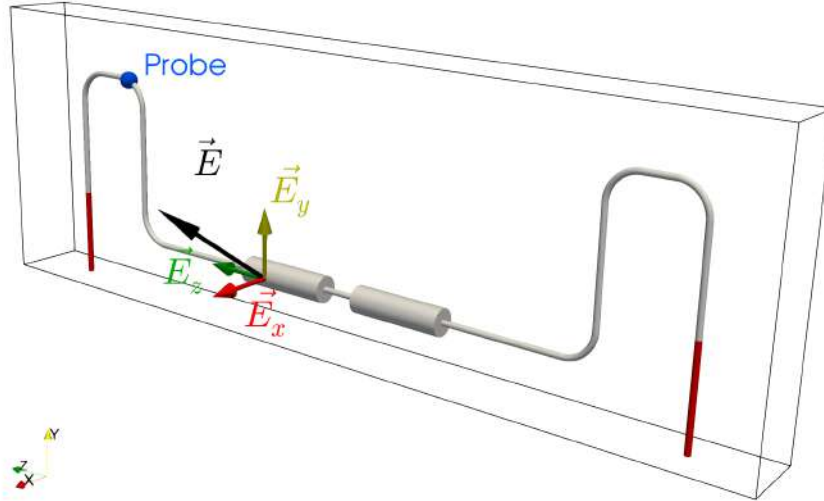


Figure 3: Illustration of point where the force is applied and the position of the probe used.

Table 1: Boundary condition for the fluid subsystem.

Position of the boundary	Velocities [$m s^{-1}$] and Gradients [s^{-1}]			Pressure [Pa] and Gradients [$Pa m^{-1}$]
	u	v	w	
X_{min} (Neumann)	$\frac{\partial u}{\partial x} = 0, 0$	$\frac{\partial v}{\partial x} = 0, 0$	$\frac{\partial w}{\partial x} = 0, 0$	$p = 0, 0$
X_{max} (Neumann)	$\frac{\partial u}{\partial x} = 0, 0$	$\frac{\partial v}{\partial x} = 0, 0$	$\frac{\partial w}{\partial x} = 0, 0$	$p = 0, 0$
Y_{min} (Dirichlet)	$u = 0, 0$	$v = 0, 0$	$w = 0, 0$	$\frac{\partial p}{\partial y} = 0, 0$
Y_{max} (Neumann)	$\frac{\partial u}{\partial y} = 0, 0$	$\frac{\partial v}{\partial y} = 0, 0$	$\frac{\partial w}{\partial y} = 0, 0$	$p = 0, 0$
Z_{min} (Neumann)	$\frac{\partial u}{\partial z} = 0, 0$	$\frac{\partial v}{\partial z} = 0, 0$	$\frac{\partial w}{\partial z} = 0, 0$	$p = 0, 0$
Z_{max} (Neumann)	$\frac{\partial u}{\partial z} = 0, 0$	$\frac{\partial v}{\partial z} = 0, 0$	$\frac{\partial w}{\partial z} = 0, 0$	$p = 0, 0$

Table 2: Initial condition for the fluid subsystem.

	Velocities [$m s^{-1}$]			Pressure [Pa]
	u	v	w	
Initial condition	0,0	0,0	0,0	0,0

at the surface of the pipe matches the structure velocity itself, given by the structure finite element model at the time analyzed.

2.3 Numerical model

In the numerical model, the problem formulation under study is presented taking into account the simplifications discussed in the physical model and in the mathematical model represented by differential equations. The numerical methods used to obtain the discretized equations of the fluid and the structure subsystems are presented next.

2.3.1 Fluid subsystem

The numerical method chosen for solving the momentum and Poisson equations for pressure correction is based on a three-dimensional, staggered, finite-volume discretization with adaptive mesh refinement, as can be seen on Figure 4.

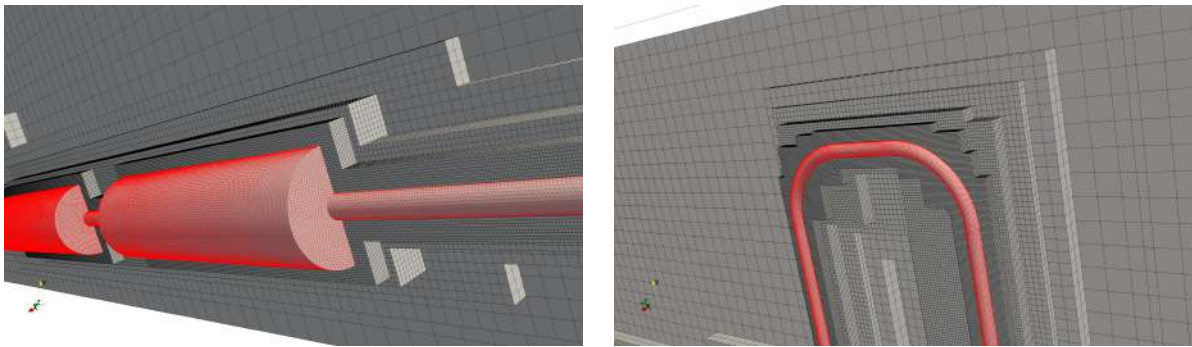


Figure 4: Illustration of structured adaptive mesh refinement with IBM used.

The central difference scheme (CDS) is applied to discretize the diffusive contributions of the transport equations. For the advective terms, the discretization was performed with Barton's method for monotonic transport as presented in Centrella and Wilson (1984). This method is a Total Variation Diminished (TVD) scheme, which is a concept introduced in Harten (1997). This is an important property of a discretization method for advective terms, as it helps to control and prevent numerical instabilities. A semi-implicit approach using the Semi-implicit Backward Differentiation Formula (SBDF) scheme has been adopted Wang and Ruuth (2008), and the resulting linear systems are solved using the geometric multigrid multilevel solver for velocity components. Since the numerical code developed adopts a pressure-velocity coupling based on pressure variations, an appropriate algorithm for pressure-velocity coupling is needed. Here, a projection method based on the fractional steps technique Chorin (1967) is used, resulting in a variable-coefficient Poisson equation which is solved with the geometric multigrid multilevel solver.

2.3.2 The Immersed Boundary Method

The immersed boundary method is necessary to impose the boundary condition on the fluid subsystem at the fluid-structure interface. In addition, it is used to determine the fluid dynamics forces acting on the structure.

The immersed boundary method used here is an adaptation of that of Wang *et al.* (2008).

The fluid domain is discretized in a uniform Cartesian mesh, while the surface of the structure is represented by Lagrangian points. These points move within the fluid domain. This movement is prescribed by the structure movement. The fluid velocity at the Lagrangian points (the interface between the fluid and the structure) should be equal to the velocity of the material points which belong to the structure. Both the velocity and position of these Lagrangian points are variable in time. Therefore, it is necessary to use a method that locates the Lagrangian points in the fluid domain and imposes the local velocity of the structure on the fluid. The surface of the Spool is discretized in 198,124 Lagrangian points represented by the same number of triangles given in an STL file Vedovoto *et al.* (2015). This quantity remains constant in the course of the simulation.

2.3.3 Structure subsystem

In this section, the discretized equations of a Timoshenko beam are presented in the physical domain.

The pipe is modeled as a circular cross-section beam with constant internal and external diameters. The finite element discretized equations are based on Cavalini (2013). In the case of the structure subsystem, the finite element discretized equations are obtained from the evaluation of the kinetic and potential energies of the beam elements. Here, the elementary stiffness matrix takes into account the increase of stiffness due to an imposed axial force.

The resulting system of global equations can be written as:

$$M_G \ddot{q} + C_G \dot{q} + K_G q = W + F, \quad (3)$$

where M_G is the global mass matrix, C_G is the global damping matrix, and K_G is the global stiffness matrix. The vector of displacements is represented by q and the weight by W . F represents the fluid dynamics forces. The damping matrix C_G is expressed as a linear combination of the mass and stiffness matrices:

$$C_G = \gamma M + \beta K, \quad (4)$$

where γ and β must be assumed. The adopted values are $\gamma = 1.0 \times 10^{-3}$ and $\beta = 1.0 \times 10^{-7}$. This assumption, although common in forced vibrations, is rather problematic for problems of stability. For these problems, the stability can be extremely sensitive to the structure damping matrix Hagedorn *et al.* (2014, 2015).

It was used the conversion of the second-order system of ordinary differential equations (ODEs), described in physical coordinates, to modal coordinates which are also time-dependent Rao (2009); Maia *et al.* (2003). In order to numerically solve the resultant set of ODEs, the state-space form was used to reduce the order of the ODEs from second to first order. In the present paper, the Runge–Kutta–Fehlberg integrator is used to numerically integrate the resultant system of equations. The dynamic models represented in state-space and some related subjects are treated in detail in Ogata (1998).

The initial condition is imposed using:

$$\begin{aligned} q &= K_G^{-1} W, \\ \dot{q} &= 0.0. \end{aligned} \quad (5)$$

The support conditions are modeled as linear springs with an elastic constant of $1 \times 10^{10} \text{ N m}^{-1}$. Those springs are imposed on all the degrees of freedom of the node chosen to model the support condition.

2.3.4 Fluid–structure coupling

In Sections 2.3.1 and 2.3.3 there was presented the numerical methods used for the computation of the solutions for the fluid and structural subdomains, respectively. It is now necessary to couple the subsystems so that the complete solution of the fluid–structure interaction problem can be achieved. There are basically two ways of coupling the subsystems. The monolithic coupling (outside the scope of the present paper) and partitioned coupling Sotiropoulos and Yang (2014). In the monolithic coupling, the fluid and structure subsystems are treated as a single nonlinear system, while in the partitioned coupling, the equations are solved separately.

We use the strong coupling, that is a type of partitioned coupling, which consists of treating the fluid subsystem with the frame position and velocity at the time n (D^n), obtaining the force acting on the structure at time $n + 1$ (F_k^{n+1}). With this force, the structure subsystem is then solved, obtaining D_k^{n+1} . This position and velocity are then used to solve the equations for the fluid subdomain and obtain F_{k+1}^{n+1} , and so on. This process will continue, until the residue of force, displacement and velocity reach a tolerance. Then, this process will be repeated on time $n + 2$.

This type of coupling has an error of $\mathcal{O}(\Delta t^{\min(p,q)})$, according to Matthies *et al.* (2006), where p and q are the order of accuracy of the time integrator of the fluid and the structure respectively. In addition, according to Förster *et al.* (2006), when used in an incompressible flow formulation, it presents a better stability when compared with the weak coupling.

3. RESULTS AND DISCUSSIONS

In this section the results obtained by the pluck test described in the section above are presented. The first results shown here are the spool's vibration modes. For simplicity only the first six modes are depicted. In figure 5 the spool's fixed part is colored in red, the initial condition is black and the vibrating mode is green.

Secondly the instantaneous force is applied to the structure and the displacement signal from the probe is acquired in each time step. The simulation was set to run 20 physical seconds, and the FRF using displacement and force signals is then performed. In figure 6 both displacements and frequencies can be seen for each direction, and the FRF peaks are labeled to provide easy identification.

Table 3 show the comparison between the measured frequencies on the submerged spool and the theoretical vacuum frequencies calculated by solving the eigenproblem for the structure alone. As expected the frequencies in water are lower than in vacuum.

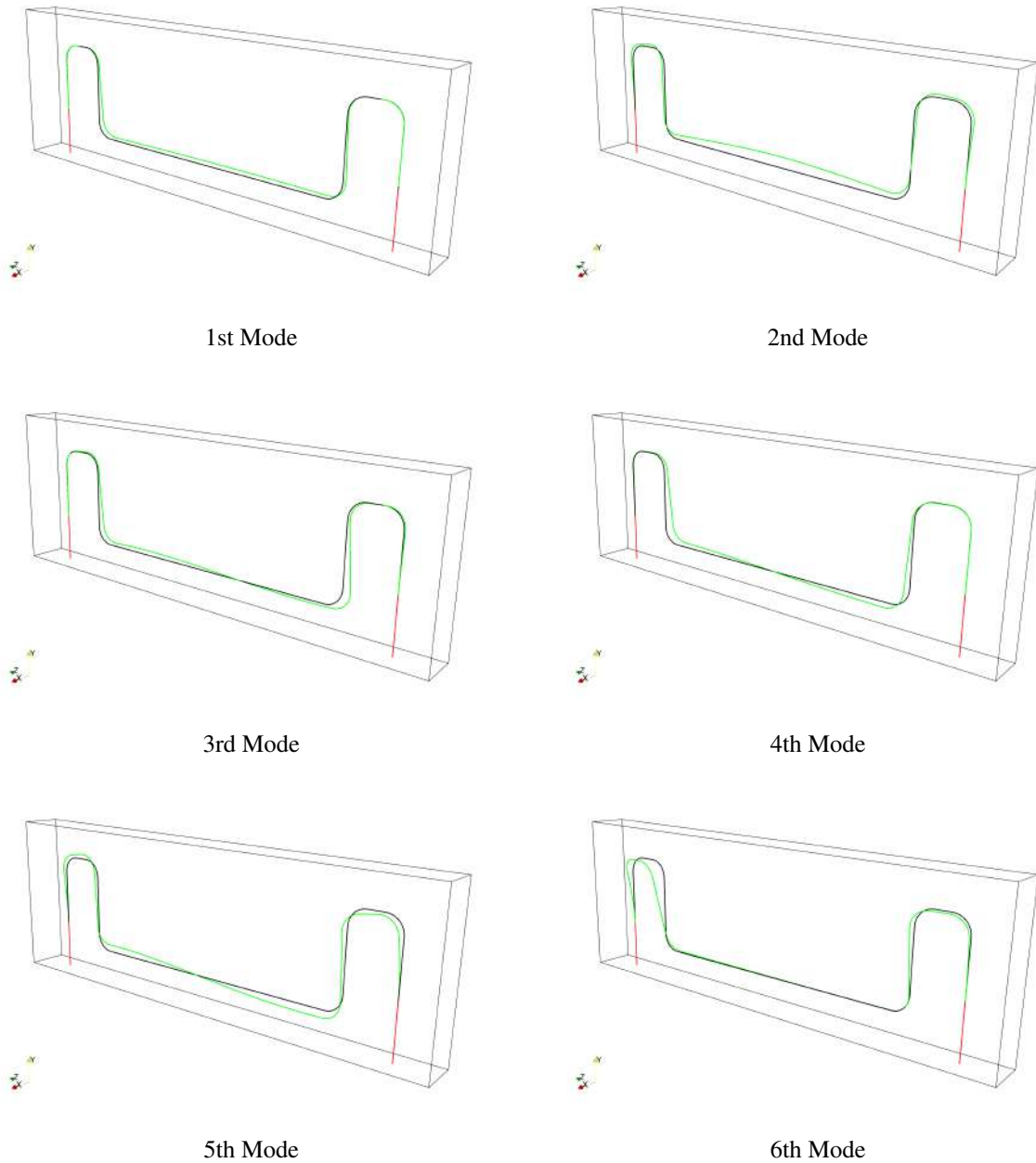


Figure 5: Vibrating mode shapes.

Table 3: Comparison of natural frequencies in vacuum and submerged in water.

Mode	Vacuum [Hz]	Water [Hz]
1	0.45	0.25
2	1.01	0.45
3	1.09	0.65
4	1.12	0.85
5	1.67	1.25
6	1.94	1.70
7	2.21	1.80
8	2.23	1.95
9	2.57	2.05
10	5.01	2.55
11	5.02	2.90

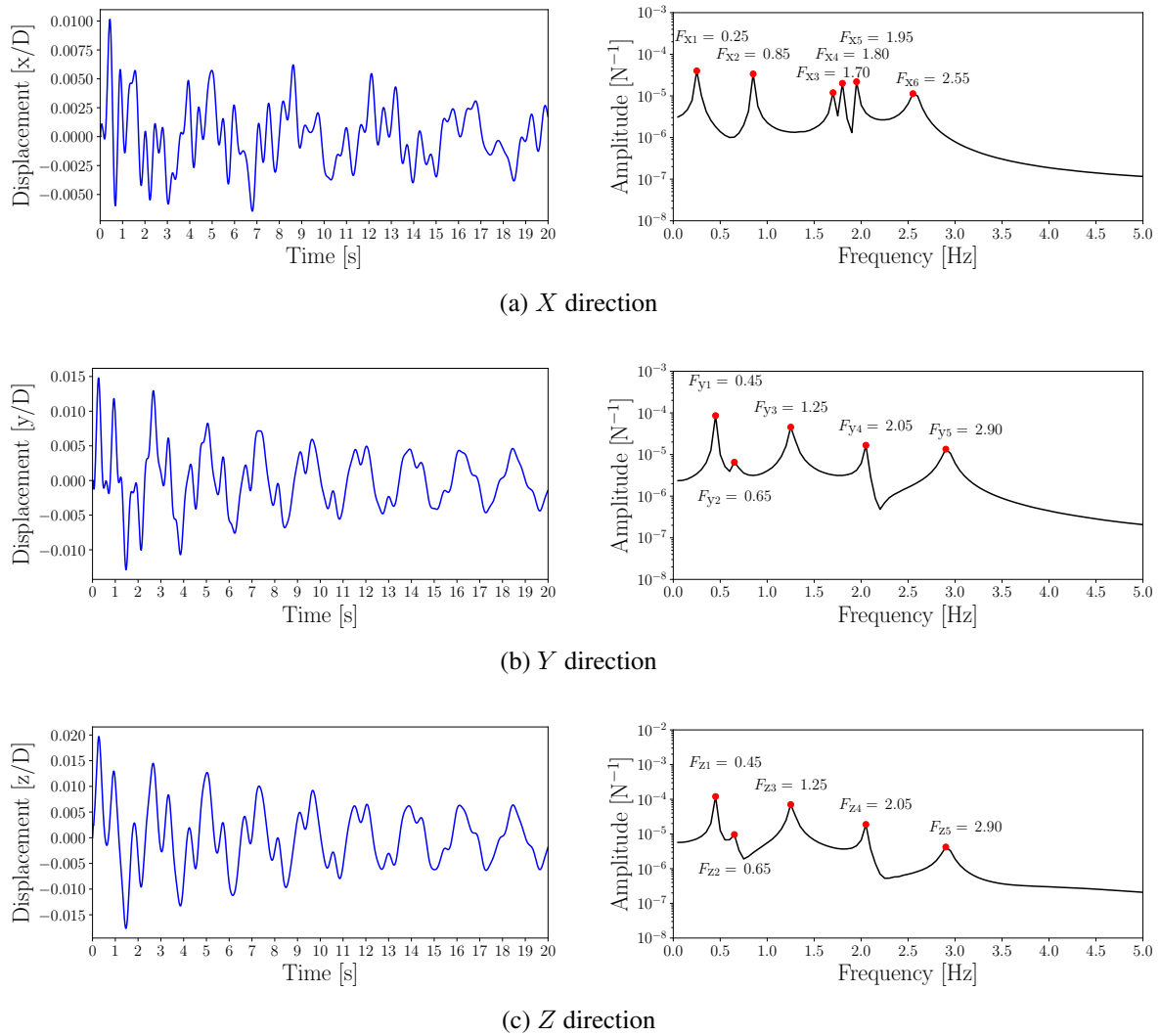


Figure 6: Dimensionless displacements and FRF results.

4. CONCLUSIONS

The present paper performed an analysis that can be considered a numerical experiment, since it reproduces what would be done in a material experiment using a water tank and a spool model, although the present method is numerical and consequently cheaper.

In the simulations performed, the natural frequencies of the spool submerged in water are found without the insertion of any ad hoc constants or added mass methods, therefore the proposed methodology can be considered generic. The simulations were possible by using the parallel in-house code MFSim with 12 processors and lasted through 8.65 hours until the results were obtained.

5. ACKNOWLEDGEMENTS

The authors are thankful to the Brazilian Research Agencies FAPEMIG and CNPq (INCT-EIE) and to CAPES and Petrobras S.A. for the financial support provided for this research.

6. REFERENCES

- Bruschi, R., Bartolini, L., Molinari, C., Vignati, G.C. and Vitali, L., 2015. "VIV Basics for Subsea Spool/Jumper Design". In *International Conference on Offshore Mechanics and Arctic Engineering, Volume 5A: Pipeline and Riser Technology*. ASME. doi:10.1115/OMAE2015-41094.
- Cavalini, A.A., 2013. *Deteção e Identificação de Trincas Transversais Iniciais em Eixos Horizontais Flexíveis de Máquinas Rotativas*. Doctoral thesis, Universidade Federal de Uberlândia, Minas Gerais, Brazil.
- Centrella, J. and Wilson, J.R., 1984. "Planar numerical cosmology. II - The difference equations and numerical tests".

The Astrophysical Journal Supplement Series, Vol. 54, pp. 229–249. doi:10.1086/190927.

- Chorin, A.J., 1967. “The numerical solution of the navier-stokes equations for an incompressible fluid”. *Bull. Amer. Math. Soc.*, Vol. 73, No. 6, pp. 928–931. URL <http://projecteuclid.org/euclid.bams/1183529112>.
- Damasceno, M., Vedovoto, J. and Da Silveira-Neto, A., 2015. “Turbulent inlet conditions modeling using large-eddy simulations”. Vol. 104, pp. 105–132.
- Förster, C., Wall, W.A. and Ramm, E., 2006. “The artificial added mass effect in sequential staggered fluid-structure interaction algorithms”. *European Conference on Computational Fluid Dynamics ECCOMAS CFD 2006*.
- Hagedorn, P., Eckstein, M., Heffel, E. and Wagner, A., 2014. “Self-Excited Vibrations and Damping in Circulatory Systems”. *Journal of Applied Mechanics*, Vol. 81, No. 10, pp. 1–9. ISSN 0021-8936. doi:10.1115/1.4028240.
- Hagedorn, P., Heffel, E., Lancaster, P., Müller, P.C. and Kapuria, S., 2015. “Some recent results on MDGKN-systems”. *ZAMM Zeitschrift für Angewandte Mathematik und Mechanik*, Vol. 95, No. 7, pp. 695–702. ISSN 15214001. doi: 10.1002/zamm.201300270.
- Harten, A., 1997. “High Resolution Schemes for Hyperbolic Conservation Laws”. *Journal of Computational Physics*, Vol. 135, pp. 260–278. doi:10.1006/jcph.1997.5713.
- Maia, N., Silva, J., Almas, E. and Sampaio, R., 2003. “Damage detection in structures: From mode shape to frequency response function methods”. *Mechanical Systems and Signal Processing*, Vol. 17, No. 3, pp. 489–498. ISSN 0888-3270. doi:<http://dx.doi.org/10.1006/mssp.2002.1506>. URL <http://www.sciencedirect.com/science/article/pii/S0888327002915062>.
- Matthies, H.G., Niekamp, R. and Steindorf, J., 2006. “Algorithms for strong coupling procedures”. *Computer Methods in Applied Mechanics and Engineering*, Vol. 195, No. 17–18, pp. 2028–2049. ISSN 0045-7825. doi:<http://dx.doi.org/10.1016/j.cma.2004.11.032>. URL <http://www.sciencedirect.com/science/article/pii/S0045782505001969>.
- Ogata, K., 1998. *Engenharia de controle moderno*. Prentice-Hall.
- Rao, S., 2009. *Vibrações mecânicas*. Prentice-Hall. ISBN 9788576052005. URL <https://books.google.com.br/books?id=3DSNPgAACAAJ>.
- Sotiropoulos, F. and Yang, X., 2014. “Immersed boundary methods for simulating fluid–structure interaction”. *Progress in Aerospace Sciences*, Vol. 65, pp. 1–21.
- Vedovoto, J.M., Serfaty, R. and Silveira Neto, A.d., 2015. “Mathematical and numerical modeling of turbulent flows”. *Anais da Academia Brasileira de Ciências*, Vol. 87, pp. 1195 – 1232. ISSN 0001-3765.
- Wang, D. and Ruuth, S., 2008. “Variable step-size implicit-explicit linear multistep methods for time-dependent partial differential equations”. *Journal of Computational Mathematics*, Vol. 26, pp. 838–855. URL <http://hdl.handle.net/2142/18708>.
- Wang, Z., Fan, J. and Luo, K., 2008. “Combined multi-direct forcing and immersed boundary method for simulating flows with moving particles”. *International Journal of Multiphase Flow*, Vol. 34, No. 3, pp. 283–302. ISSN 0301-9322. doi:<http://dx.doi.org/10.1016/j.ijmultiphaseflow.2007.10.004>. URL <http://www.sciencedirect.com/science/article/pii/S0301932207001474>.

7. RESPONSIBILITY NOTICE

The authors are the only responsible for the printed material included in this paper.